10 December 1999

ELSEVIER

Chemical Physics Letters 314 (1999) 435–442

CHEMICAL PHYSICS LETTERS

www.elsevier.nl/locate/cplett

On the formation of benzene oxide/oxepin in the gas-phase reaction of OH radicals with benzene

T. Berndt *, O. Böge, H. Herrmann

Institut für Troposphärenforschung e.V., Permoserstraße 15, 04303 Leipzig, Germany

Received 2 August 1999; in final form 3 September 1999

Abstract

Product formation in the gas-phase reaction of OH radicals with benzene was studied under flow-tube conditions at 13 and 100 mbar at 298 K in O_2/He mixtures using direct MS, on-line FT-IR spectroscopy and GC-MS/FID detection. Benzene was used in a large excess, preventing consecutive reactions of products. Under all experimental conditions investigated there was no clear indication for a formation pathway for benzene oxide/oxepin; the observed yield was < 0.03 (FT-IR) and < 0.01 (GC-MS). Observed products were CO: 0.30 ± 0.13, phenol: 0.23 ± 0.07, formic acid: 0.13 ± 0.05, *p*-benzoquinone: 0.055 ± 0.009, and unidentified carbonyls: 0.59 ± 0.11 (yields at 100 mbar).

1. Introduction

Especially in urban areas, benzene and its alkylated derivatives (toluene, ethylbenzene, xylenes) represent one of the most abundant hydrocarbons in the troposphere. Their degradation in the gas phase is exclusively initiated by the attack of OH radicals. Although in the last 20 years the atmospheric chemistry of benzene has been intensively studied there is no clarity concerning the product distribution [1].

For benzene, the initial attack of OH radicals proceeds by addition and the H-atom abstraction pathway is negligible under tropospheric conditions [2–4]. The formed hydroxycyclohexadienyl radical (HCHD) is resonance-stabilized and the fate of this species in the troposphere has been subject of various kinetic studies concerning its reaction with O_2, NO and NO_2 [5–7]. Although there are discrepancies for the reaction of HCHD with O_2 [6,7], these studies showed that under conditions close to those of the real troposphere, the fate of HCHD is governed by its reaction with O_2. From a mechanistic point of view, this reaction pathway may represent an addition step as well as a H-atom abstraction. This latter process has been suggested to explain the formation of benzene oxide by H-atom abstraction at the hydroxyl position of HCHD [8], cf. pathway (1):

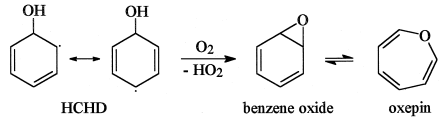

(1)

From experiments in solution it is known that benzene oxide is in equilibrium with its isomeric species oxepin [9]. By analogy, for the gas phase the same

* Corresponding author. Fax: +49-341-2352325; e-mail: berndt@tropos.de

0009-2614/99/$ - see front matter
PII: S0009-2614(99)01041-6

behavior is expected [10]. The concept of arene oxide formation has been suggested by Shepson et al. as a result of a product study of the gas-phase reaction of OH radicals with *o*-xylene [11]. For the benzene reaction, the experimental finding that HO_2 rather than DO_2 is formed in the reaction of OH radicals with benzene-d_6 was taken as an argument for a possible formation of benzene oxide/oxepin [12]. According to a theoretical investigation of the reaction of HCHD with O_2, the formation of benzene oxide/oxepin via pathway (1) is not favorable compared to (i) phenol formation by H-atom abstraction from the hydroxylated carbon atom, or (ii) the addition pathway leading to a hydroxycyclohexadienyl peroxyl radical (HCHD-O_2) [13]. Although there is no experimental evidence for the formation of benzene oxide/oxepin via pathway (1) the atmospheric chemistry of these compounds has recently been investigated [10,14].

Because of the currently speculative nature of pathway (1) more experimental work is needed for a better understanding of the atmospheric fate of HCHD. The aim of the present investigation is to find out whether or not benzene oxide/oxepin is formed as a stable product in the reaction of OH radicals with benzene.

2. Experimental

The schematic of the experimental arrangement is shown in Fig. 1. The experiments have been performed at $T = 298$ K at 13 or 100 mbar in different He/O_2 mixtures. OH radicals were produced via the reaction sequence $H + O_2 \rightarrow HO_2$; $H + HO_2 \rightarrow 2OH$ in a pre-reactor. The H atoms needed were generated

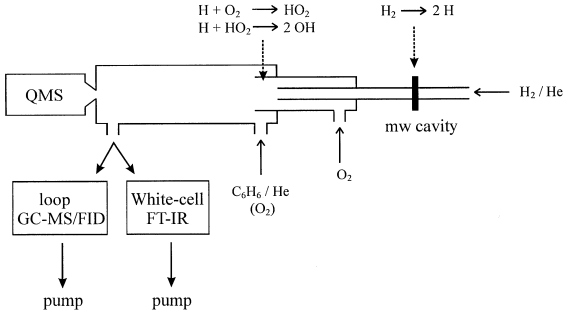

Fig. 1. Schematic of the experimental arrangement.

in a 0.8 cm i.d. moveable duran-glass tube by means of a microwave discharge (SAIREM GMP 03 K/SM) operating at 70 W using 0.07–0.47% H_2 diluted in He. In the pre-reactor (1.15 cm i.d. quartz glass) attached on the main tube (2.0 cm i.d. quartz glass) the H atoms were mixed with O_2 ($[O_2] = (4.8–12) \times 10^{16}$ molecule cm^{-3}) finally generating the OH radicals. After a residence time of ca. 0.01 s the gas mixture was introduced into the main tube where it was mixed with benzene diluted in He as well as additional O_2.

Typical conditions in the main tube were: $[O_2] = 1.0 \times 10^{17}$ molecule cm^{-3} at a total pressure of 13 mbar and 1.6×10^{18} molecule cm^{-3} at 100 mbar, $[C_6H_6] = (3.2–7.8) \times 10^{15}$ molecule cm^{-3} and a bulk velocity $v = 1.3–2.1$ m s^{-1} resulting in a residence time of 0.26–0.42 s. The pressure in the main tube was measured by capacitive manometers (Baratron). All gas flows were set by calibrated mass flow controllers (MKS 1259).

At the outlet of the main tube a quadrupole mass spectrometer (Balzers QMA 200) was attached working in the 70 eV electron impact mode. The predominant part of the reaction gas was pumped continuously through a 2050 cm^3 cell with a White cell mirror system (optical path length 10 m). FT-IR spectra were recorded with an instrumental resolution of 8 cm^{-1} using a MCT detector by coadding of 200–2000 scans (Nicolet Magna 750). The following substances were identified by characteristic band locations and the concentrations were determined using calibrated spectra of authentic samples measured under reaction conditions: CO: 2123 and 2172 cm^{-1}; benzene: 1483 and 3048 cm^{-1}; phenol: 1607 and 3650 cm^{-1}; formic acid: 1761 and 1791 cm^{-1}; benzene oxide/oxepin: 1084 and 3048 cm^{-1}. Note, in agreement with earlier observations [15], the absorption cross section for CO was found to be concentration dependent. Furthermore, the signals for CO were close to the detection limit preventing a precise CO determination. Because of their very low vapor pressure, the reference spectra of *cis,cis*-2,4-hexadienedial (1570 and 1703 cm^{-1}) and *p*-benzoquinone (1680 cm^{-1}) were recorded under vacuum conditions. A determination of the absorption cross section was impossible. For the latter compound a value from the structurally similar *cis*-butenedial was used [16]. Averaged integrated band intensities (IBI)

from methyl vinyl ketone, methacrolein and methyl ethyl ketone which are in reasonable agreement were taken for quantification of unidentified carbonyls.

Furthermore, a small gas stream was pumped continuously through two GC loops for MS and FID analysis (HP 5890 with HP-MSD 5971) using an additional pump system. The loops were directly connected with the outlet of the main tube by a transfer line. In order to reduce wall loss effects the GC loops as well as the transfer line was heated up to 373 K. For product separation 30 m, 0.25 mm i.d. capillary columns (HP 5MS) were chosen.

The gases used had stated purities as follows: He (99.999%), O_2 (99.9995%), and H_2 (99.999%) (Messer Griesheim). For further purification, the gases were passed through an active carbon trap maintained at dry-ice temperature. Benzene oxide/oxepin was prepared according to the method of Gillard et al. [17]. *cis,cis*-2,4-hexadienedial was synthesized by $NaIO_4$ oxidation of *cis*-3,5-cyclohexadiene-1,2-diol (Fluka) [18]. Phenol (> 99.99%), benzene (> 99.9%) (Aldrich) and *p*-benzoquinone (99.5%) (Fluka) were used as purchased. Formic acid (98%) (Fluka) was dried ($CuSO_4$) just before use. Purities were checked by GC-MS/FID. The only detectable impurity for benzene was methylcyclohexane (< 0.01%).

2.1. OH formation in the pre-reactor

The reaction of H atoms produced in a microwave discharge with O_2 occurs according to the sequence

$$H + O_2 + M \rightarrow HO_2 + M \quad (2)$$

$$H + HO_2 \rightarrow 2OH \quad (0.87 \pm 0.04) \quad (3a)$$

$$H + HO_2 \rightarrow H_2O + O \quad (0.04 \pm 0.02) \quad (3b)$$

$$H + HO_2 \rightarrow H_2 + O_2 \quad (0.09 \pm 0.04) \quad (3c)$$

with k_2 $(M = N_2) = 6.1 \times 10^{-32}$ cm^6 molecule^{-2} s^{-1} [19] (value for N_2 here applied for the O_2/He mixture) and $k_3 = 7.5 \times 10^{-11}$ cm^3 molecule^{-1} s^{-1} [19]. The branching ratios for the pathways (3a)–(3c) were taken from an experimental study performed under similar reaction conditions [19]. For an estimation of the concentration levels of all reactive species in the pre-reactor (OH, O, H, HO_2) the overall reaction was modeled considering the following additional pathways [19]

$$OH + HO_2 \rightarrow H_2O + O_2 \quad (4)$$

$$OH + OH \rightarrow H_2O + O \quad (5)$$

$$O + OH \rightarrow H + O_2 \quad (6)$$

$$O + HO_2 \rightarrow OH + O_2 \quad (7)$$

with $k_4 = 7.0 \times 10^{-11}$, $k_5 = 1.8 \times 10^{-12}$, $k_6 = 3.3 \times 10^{-11}$, $k_7 = 5.4 \times 10^{-11}$ (all in units: cm^3 molecule^{-1} s^{-1}) as well as the wall loss for the radicals assuming first-order rate constants of 10 s^{-1} for OH, O and HO_2 and 2 s^{-1} for H. For typical reaction conditions ($p = 13$ mbar, $[O_2] = 1.2 \times 10^{17}$ molecule cm^{-3}, $[H] = 1.0 \times 10^{14}$ molecule cm^{-3}, $t = 0.01$ s), the OH radicals formed represent the predominant fraction of the radicals. The concentration of H atoms is negligible and O atoms as well as HO_2 radicals are of even less importance, for this example: $[OH]/[O]/[HO_2]/[H] = 1/0.066/0.035/0.007$.

To check this with special attention to the formed O atoms, titration experiments using tetramethylethylene (TME) were undertaken. Product studies of the reaction of O atoms ($O(^3P)$) with TME in O_2/He mixtures were subject of earlier investigations in this laboratory,

$$O + TME \rightarrow \text{products} \quad (8)$$

($k_8 = 6.8 \times 10^{-11}$ cm^3 molecule^{-1} s^{-1} [20]). As the main products tetramethyloxirane (yield: 0.42 ± 0.05) and pinacolone (yield: 0.30 ± 0.04) were identified [21], $p = 50$ mbar and $[O_2] = (1.1–14) \times 10^{16}$ molecule cm^{-3}. On the other hand, the main product of the reaction of OH radicals with TME

$$OH + TME \rightarrow \text{products} \quad (9)$$

($k_9 = 10.8 \times 10^{-11}$ cm^3 molecule^{-1} s^{-1} [22]), is acetone with a yield of 1.6–1.7 [23]. No experimental indication for the formation of tetramethyloxirane or pinacolone exists. Therefore, under reaction conditions ($p = 13$ mbar, $[O_2] = 1.0 \times 10^{17}$ molecule cm^{-3}, $[TME] = 3.7 \times 10^{13}$ molecule cm^{-3}) TME was introduced instead of benzene and the formation yield of tetramethyloxirane with respect to reacted TME was determined to be 0.027 ± 0.007 using GC-MS and GC-FID analysis. Assuming that only O

atoms and OH radicals reacted with TME a content of $6 \pm 2\%$ O atoms and $94 \pm 2\%$ OH radicals follows to be in a good agreement with the modeling results.

2.2. Consecutive reactions

In order to avoid the consecutive reactions of OH radicals with all products, only 0.07–0.25% of the initial benzene concentration (measured by FT-IR) was converted

$$OH + C_6H_6 \rightarrow \text{products (HCHD)} \quad (10)$$

($k_{10} = 1.23 \times 10^{-12}$ cm^3 molecule^{-1} s^{-1} [1]). Assuming a rate constant of 1×10^{-10} cm^3 molecule^{-1} s^{-1} for the generalized reaction of OH radicals with products, more than 90% of the OH radicals reacted via pathway (10).

3. Results

3.1. Direct MS analysis

Because of limited pump efficiency of the used MS equipment, experiments were only performed at a total pressure of 13 mbar. Difference spectra as well as ion traces were recorded with and without OH-radical production (turn on/off the stream of H_2 or the microwave discharge). Clear product signals observed at $m/z = 29$, 45 and 94 amu were assigned to the ions (CHO^+), (CHO_2^+) and ($C_6H_6O^+$), respectively. A typical temporal behavior of the ion traces is given in Fig. 2 ($[O_2] = 1.0 \times 10^{17}$ molecule cm^{-3}, $[C_6H_6] = 7.8 \times 10^{15}$ molecule cm^{-3}, $\Delta[C_6H_6] = 1.8 \times 10^{13}$ molecule cm^{-3}). The reference mass spectrum of benzene oxide/oxepin shows the strongest signals at $m/z = 66$ and 94 amu. For $m/z = 66$ amu there was no clear indication in the product spectrum. Furthermore, phenol (also C_6H_6O) was formed in substantial fraction and the observed signal at $m/z = 94$ amu was, at least in part, due to this compound. Therefore, it must be concluded that benzene oxide/oxepin does not represent a main product. On the other hand, the signals at $m/z = 29$ and 45 amu can be attributed to aldehydes and carboxylic species to be formed in considerable amounts.

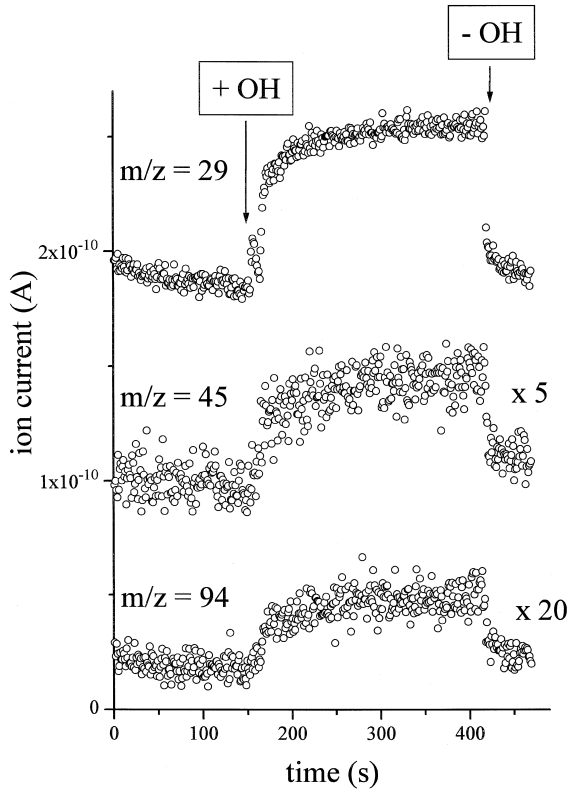

Fig. 2. Observed ion traces from direct MS analysis with and without OH-radical formation in the pre-reactor at $m/z = 29$, 45 and 94 amu assigned to (CHO^+), (CHO_2^+) and ($C_6H_6O^+$), respectively.

3.2. FT-IR analysis

The reactions were conducted at $p = 13$ mbar ($[O_2] = 1.0 \times 10^{17}$ molecule cm^{-3}) or at $p = 100$ mbar ($[O_2] = 1.6 \times 10^{18}$ molecule cm^{-3}). In the recorded FT-IR spectra, in each case (35 runs) the same product absorptions were found. Fig. 3 shows the FT-IR spectrum from the run described in the MS analysis above. In the upper part the difference spectrum (H_2 turned on or off) after subtraction of H_2O bands is plotted. H_2O was formed via pathways (3b), (4) and (5) in the pre-reactor before adding benzene. The negative bands represent consumed benzene. For comparison, the reference spectrum of benzene is given in the lower part. The spectral features from 1090–1119 cm^{-1} and 1761–1791 cm^{-1} were found to be in excellent agreement

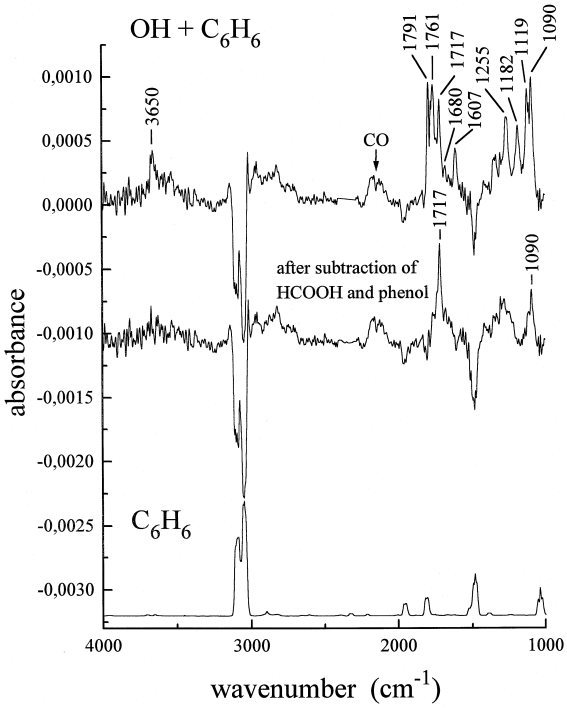

Fig. 3. Typical FT-IR difference spectrum (H_2 turned on or off) after subtraction of H_2O bands (upper part) and further subtraction of band arising from HCOOH and phenol (middle). Negative bands represent consumed benzene, for comparison the reference spectrum for benzene (lower part).

with those of formic acid (HCOOH) reference spectrum. The bands at 1182, 1255, 1607 and 3650 cm^{-1} were assigned to phenol. The small absorption at 1680 cm^{-1} was attributed to *p*-benzoquinone in accordance with the reference spectrum. Furthermore, CO was identified at 2123 and 2172 cm^{-1}.

After subtraction of HCOOH and phenol, apart from CO, bands at 1090, 1150–1350 and 1717 cm^{-1} remained. The latter band is typical for carbonylic groups in conjugation with a double bond. A possible carbonylic species discussed to be an oxidation product of benzene is the corresponding muconaldehyde [24]. Assuming that there is no isomerisation to the more stable *cis,trans*- or *trans,trans*-species, the formation of *cis,cis*-2,4-hexadienedial is expected.

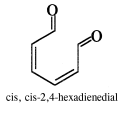

cis, cis-2,4-hexadienedial

Fig. 4 in its upper part shows the recorded reference FT-IR spectrum of this compound. Especially the location of the CO vibration disagrees with that found in the residual product spectrum. From this work there are no indications for the formation of *cis,cis*-2,4-hexadienedial and the assignment of the bands from the residual spectrum remains uncertain. Note, that the FT-IR spectrum of muconaldehyde from Fig. 4 is in good agreement with that reported in the literature [24] confirming the purity of the reference substance used here.

As a result of a chamber study the formation of glyoxal was reported [25]. In all spectra on the left side of the band centred at 1717 cm^{-1} a small shoulder at ca. 1735 cm^{-1} was visible tentatively attributed to glyoxal. Because of the low intensity a determination of the product yield was impossible. For *cis*-butenedial, the possible co-product to glyoxal, with a strong band located at 1711 cm^{-1} [16] there was no experimental evidence.

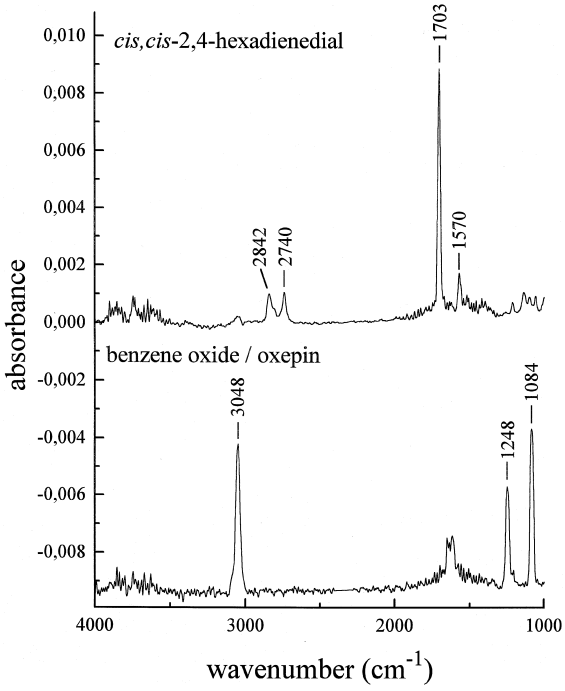

Fig. 4. Reference FT-IR spectra for the corresponding muconaldehyde *cis,cis*-2,4-hexadienedial as well as for benzene oxide/oxepin.

The lower part of Fig. 4 presents the reference FT-IR spectrum of benzene oxide/oxepin (2.2×10^{13} molecule cm^{-3}) measured under reaction conditions at $p = 13$ mbar. Taking into account that benzene oxide/oxepin contributes to the observed absorption in the residual product spectrum, cf. Fig. 3, as a result of spectral subtraction a yield < 0.03 was determined.

In Table 1 product yields with respect to consumed benzene are compiled for CO, formic acid (HCOOH), phenol (C_6H_5OH), *p*-benzoquinone ($C_6H_4O_2$) and the unidentified carbonylic compounds. Error limits given represent two standard deviations.

3.3. GC-MS analysis

Simultaneous to the FT-IR measurements, on-line GC-MS analysis was performed. The upper part of Fig. 5 shows the result of a typical run ($p = 100$ mbar, $[O_2] = 1.6 \times 10^{18}$ molecule cm^{-3}, $[C_6H_6] = 3.2 \times 10^{15}$ molecule cm^{-3}, $\Delta[C_6H_6] = 5.6 \times 10^{12}$ molecule cm^{-3}). In each run, *p*-benzoquinone and phenol were identified by means of the retention time and the mass spectra. No further noticeable signals were detected. Under reaction conditions benzene oxide/oxepin was introduced into the main tube on the port for the benzene addition. Apart from small amounts of phenol, benzene oxide/oxepin was found to be detectable with high efficiency using this analytical approach. Fig. 5 in the lower part shows the chromatogram for a tube concentration of 2.2×10^{13} molecule cm^{-3} of benzene oxide/oxepin. From direct injection of a diluted liquid sample, the peak position as well the mass spectrum was confirmed. In the analysis of the reaction products no indication for the formation of benzene oxide/oxepin exists.

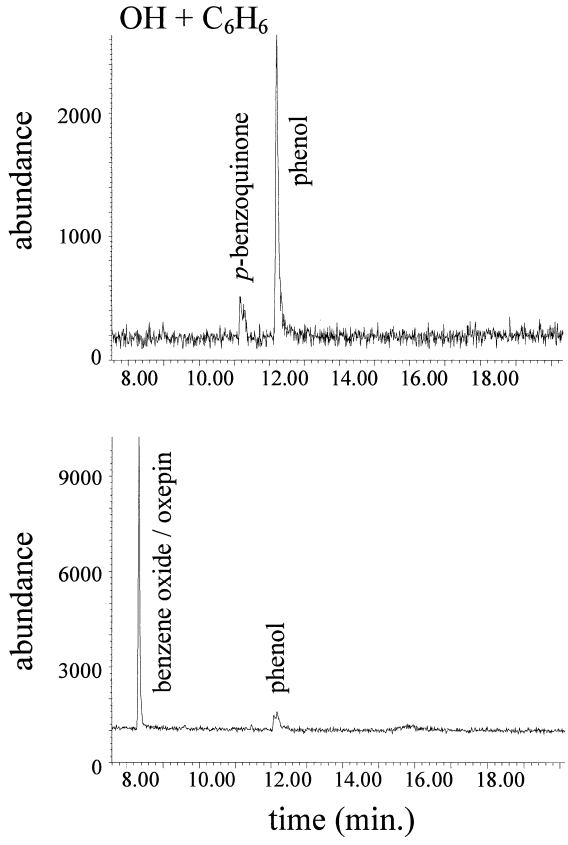

Fig. 5. Typical GC-MS run (upper part). For comparison, observed signals from an authentic sample of benzene oxide/oxepin introduced into the main tube under reaction conditions (lower part).

This leads to a benzene oxide/oxepin upper limit yield < 0.01.

4. Discussion

The primary intention of this work was to find out if benzene oxide is formed in a reaction of HCHD

Table 1
Determined product yields[a] (error limits represent two standard deviations)

p (mbar)	$[O_2]$ (cm^{-3})	$\Delta[C_6H_6]$ (cm^{-3})	CO	HCOOH	C_6H_5OH	$C_6H_4O_2$	Carbonyls[b]
13	1.0×10^{17}	$(5.3–20) \times 10^{12}$	0.42 ± 0.22	0.16 ± 0.03	0.24 ± 0.08	0.026 ± 0.003	0.42 ± 0.15
100	1.6×10^{18}	$(3.5–5.9) \times 10^{12}$	0.30 ± 0.13	0.13 ± 0.05	0.23 ± 0.07	0.055 ± 0.009	0.59 ± 0.11

[a] Yields obtained with respect to consumed C_6H_6.
[b] Formed carbonyl groups per consumed C_6H_6.

with O_2 by H-atom abstraction via pathway (1) or not. In agreement with theoretical predictions concerning the reaction of HCHD with O_2 [13], these experiments do not show benzene oxide/oxepin formation. Instead, CO, formic acid, phenol, *p*-benzoquinone, tentatively glyoxal and other (at present unidentified) carbonyls were detected.

The observed phenol yield from this study, 0.24 ± 0.08 (13 mbar) and 0.23 ± 0.07 (100 mbar), is in excellent agreement with that obtained in a chamber study in air, 0.236 ± 0.044 [26], as well as from a radiolysis experiment in the absence of O_2, 0.25 ± 0.05 [7]. From the experiments described here, it is impossible to decide if phenol is formed in a direct way from the reaction of OH radicals with benzene [7] or from the reaction of O_2 with HCHD as often described in the literature.

The formation of CO, formic acid and *p*-benzoquinone from the reaction of OH radicals with benzene is reported here for the first time. However, CO, formic acid and the corresponding 4-methyl-*p*-benzoquinone has been found as products of the more comprehensively investigated reaction of OH radicals with toluene [27,28]. Proposed formation pathways for these compounds involving intramolecular O_2 bridged methyl-hydroxycyclohexadienyl radicals are also applicable for the benzene system. Nevertheless, it appears to be highly speculative to suggest a detailed mechanism for the formation of CO, formic acid and *p*-benzoquinone as a result of this study.

The significantly higher product yield for *p*-benzoquinone as well as the increased carbonyl yield at $p = 100$ mbar relative to the measurement at $p = 13$ mbar can be attributed to lower wall losses of precursor species or the products itself. On the other hand, at a total pressure of 100 mbar the O_2 concentration was increased by a factor of 16 relative to the lower total pressure of 13 mbar. Therefore, this observed effect for *p*-benzoquinone and the carbonyls can be explained also by a more dominant reaction of HCHD or other intermediates with O_2 at the higher O_2 concentration.

Besides phenol, carbonylic compounds represent the main fraction of the identified products. In the literature currently only the formation of glyoxal with a yield of 0.207 ± 0.019 is reported [25]. As a result of FT-IR studies of the present experiments, an observed small shoulder at ca. 1735 cm^{-1} on the carbonylic band centred at 1717 cm^{-1} was tentatively attributed to glyoxal. Because of the low intensity a determination of the product yield was impossible. For *cis*-butenedial, a possible co-product to glyoxal, as well as for a further carbonylic product which corresponds to benzene ring-cleavage, *cis,cis*-2,4-hexadienedial, there was no experimental evidence. As a result of the on-line GC-MS analysis no signals arising from carbonyls were obtained indicating very effective wall losses of these substances in the transfer line to the GC. On the other hand, the relatively strong signal at $m/z = 29$ amu observed in the direct MS analysis was assigned to the formyl ion (CHO^+) to be in line with the formation of aldehydes in considerable amounts.

4.1. Modeling

Recently, the rate constant for the self reaction of HCHD

$$HCHD + HCHD \rightarrow products \quad (11)$$

($k_{11} = 3.8 \times 10^{-11}$ cm^3 $molecule^{-1}$ s^{-1}) was communicated [29] to be much higher compared to a value which was adopted from a measurement in the liquid phase ($k_{11(liq.)} = 7.6 \times 10^{-13}$ cm^3 $molecule^{-1}$ s^{-1} [30]). Therefore, a modeling study using this new value for k_{11} was necessary to find out the impact of pathway (11) in competition to the desired reaction with O_2, i.e.

$$HCHD + O_2 \rightarrow products \quad (12)$$

($k_{12} = 2 \times 10^{-16}$ cm^3 $molecule^{-1}$ s^{-1} [6]) for the fate of HCHD under the chosen experimental conditions. For a more comprehensive discussion also the diffusion limited wall-reaction of HCHD was considered:

$$HCHD \rightarrow wall \quad (13)$$

Assuming a diffusion coefficient $D_{HCHD} = 100$ cm^2 mbar s^{-1}, by numerically solving the continuity equation for the conditions of this work first-order rate constants $k_{13} = 30$ s^{-1} ($p = 13$ mbar) and $k_{13} = 4$ s^{-1} ($p = 100$ mbar) were estimated [31]. Modeling considering pathway (10) with a HCHD formation yield of one and pathways (11), (12) and (13) was carried out for typical conditions at $p = 13$ mbar ($[O_2] = 1.0 \times 10^{17}$ molecule cm^{-3}, $[C_6H_6] = 7.8 \times$

10^{15} molecule cm^{-3}, initial $[OH] = 1.0 \times 10^{13}$ molecule cm^{-3}) and for $p = 100$ mbar ($[O_2] = 1.6 \times 10^{18}$ molecule cm^{-3}, $[C_6H_6] = 3.2 \times 10^{15}$ molecule cm^{-3}, initial $[OH] = 4.0 \times 10^{12}$ molecule cm^{-3}). Using this simple model, for conditions at $p = 13$ mbar only 7% of formed HCHD were found to be converted by the reaction with O_2 via pathway (12) and 81% by the self reaction via pathway (11). For the higher O_2 concentration at $p = 100$ mbar the reaction with O_2 dominates with 72% and in the self reaction 28% of formed HCHD were consumed. Taking into account that formic acid, *p*-benzoquinone and the carbonyls represent final products of the reaction of O_2 with HCHD, the agreement between the modeling results based on the new recombination rate constant for HCHD [29] and the experimental findings is unsatisfactory, cf. Table 1. The product studies of the present study at $p = 13$ mbar indicate a more effective reaction of O_2 with HCHD via pathway (12) in competition especially with pathway (11).

For a better understanding of the gas-phase reaction of OH radicals with benzene further kinetic and mechanistic studies are needed.

Acknowledgements

The authors thank B. Bohn and C. Zetzsch for providing results prior to publication and for helpful discussions.

References

[1] R. Atkinson, J. Phys. Chem. Ref. Data, Monograph 2 (1994) 47, and references therein.
[2] R.A. Perry, R. Atkinson, J.N. Pitts, J. Phys. Chem. 81 (1977) 296.
[3] F.P. Tully, A.R. Ravishankara, R.L. Thompson, J.M. Nicovich, R.C. Shah, N. M Kreutter, P.H. Wine, J. Phys. Chem. 85 (1981) 2262.
[4] K. Lorenz, R. Zellner, Ber. Bunsenges. Phys. Chem. 87 (1983) 629.
[5] R. Zellner, B. Fritz, M. Preidel, Chem. Phys. Lett. 121 (1985) 412.
[6] R. Knispel, R. Koch, M. Siese, C. Zetzsch, Ber. Bunsenges. Phys. Chem. 94 (1990) 1375.
[7] E. Bjergbakke, A. Sillensen, P. Pagsberg, J. Phys. Chem. 100 (1996) 5729.
[8] I. Barnes, K.H. Becker, B. Klotz, in: P.M. Borrell, P. Borrell, K. Kelly, T. Cvitas, W. Seiler (Eds.), Transport and Transformation of Pollutants in the Troposphere, Vol. 2, Computational Mechanics Publication, 1997, pp. 599–604.
[9] E. Vogel, H. Günther, Angew. Chem. 79 (1967) 429.
[10] B. Klotz, I. Barnes, K.H. Becker, B.T. Golding, J. Chem. Soc. Faraday Trans. 93 (1997) 1507.
[11] P.B. Shepson, E.O. Edney, E.W. Corse, J. Phys. Chem. 88 (1984) 4122.
[12] R. Koch, C. Zetzsch, in: P.M. Borrell, P. Borrell, K. Kelly, T. Cvitas, W. Seiler (Eds.), Transport and Transformation of Pollutants in the Troposphere, Vol. 2, Computational Mechanics Publication, 1997, pp. 477–483.
[13] G. Ghigo, G. Tonachini, J. Am. Chem. Soc. 120 (1998) 6753.
[14] B. Klotz, I. Barnes, K.H. Becker, Chem. Phys. 231 (1998) 289.
[15] C.A. Cantrell, W.R. Stockwell, L.G. Anderson, K.L. Busarow, D. Perner, A. Schmeltekopf, J.G. Calvert, H.S. Johnston, J. Phys. Chem. 89 (1985) 139.
[16] T. Berndt, O. Böge, W. Rolle, Environ. Sci. Technol. 31 (1997) 1157.
[17] J.R. Gillard, M.J. Newlands, J.N. Bridson, D.J. Burnell, Can. J. Chem. 69 (1991) 1337.
[18] B.T. Golding, G. Kennedy, W.P. Watson, Tetrahedron Lett. 29 (1988) 5991.
[19] K.J. Hsu, J.L. Durant, F. Kaufman, J. Phys. Chem. 91 (1987) 1895.
[20] R.J. Cvetanovic, J. Phys. Chem. Ref. Data 16 (1987) 261.
[21] I. Kind, unpublished results.
[22] R. Atkinson, J. Arey, S.M. Aschmann, S.B. Corchnoy, Y. Shu, Int. J. Chem. Kinet. 27 (1995) 941.
[23] E.C. Tuazon, S.M. Aschmann, J. Arey, R. Atkinson, Environ. Sci. Technol. 32 (1998) 2106.
[24] B. Klotz, A. Bierbach, I. Barnes, K.H. Becker, Environ. Sci. Technol. 29 (1995) 2322.
[25] E.C. Tuazon, H. MacLeod, R. Atkinson, W.P.L. Carter, Environ. Sci. Technol. 20 (1986) 383.
[26] R. Atkinson, S.M. Aschmann, J. Arey, W.P.L. Carter, Int. J. Chem. Kinet. 21 (1989) 801.
[27] R. Seuwen, P. Warneck, Int. J. Chem. Kinet. 28 (1996) 315, and references therein.
[28] M.W. Gery, D.L. Fox, H.E. Jeffries, L. Stockburger, W.S. Weathers, Int. J. Chem. Kinet. 17 (1985) 931.
[29] B. Bohn, C. Zetzsch, submitted for publication.
[30] S. Gordon, K.H. Schmidt, E.J. Hart, J. Phys. Chem. 81 (1977) 104.
[31] T. Berndt, R. Picht, F. Stratmann, Z. Phys. Chem. 209 (1999) 259.